ADVANCED MATERIALS
www.advmat.de

Piezoelectric Injectable Anti-Adhesive Hydrogel to Promote Endogenous Healing of Tendon Injuries

Ruizeng Luo, Yujie Xiong, Jiaxuan Li, Meng Xiao, Yuan Bai, Ziyang Xu, Zhen Luo, Cong Li, Aihua Liang, Hongqing Feng, and Zhou Li**

Achilles tendon rupture has become a common sports injury nowadays, but tendon repair is still is a challenge in the clinical practice. Tendon adhesion, which results from exogenous healing, is a crucial problem impairing tendon repair. Meanwhile, insufficient endogenous healing from the tendon stem cells, makes tendon repair even more difficult. Here, a piezoelectric injectable anti-adhesive hydrogel (PE-IAH) is reported, which can simutaneously promote endogenous healing while inhibiting exogenous healing in the tendon repair process. The in vivo study reveals that the PE-IAH can form a physical barrier in situ at the tendon injury site, which reduces the inflammatory response and effectively prevents the tendon from adhering to surrounding tissue. Meanwhile, the piezoelectric short fibers incorporated in the hydrogel can evidently promotes the proliferation and differentiation of tendon stem cells due to piezoelectric effect under ultrasound excitation. Altogethter, the PE-IAH successfully accelerates the endogenous healing of tendon in addition to the anti-adhesion purpose, resulting in remarkably elevated tendon functions (Achilles Functional Index: −15.6 of PE-IAH versus −30.6 of injectable anti-adhesive hydrogel (IAH), Day 14). This study provides a new strategy for advanced healing and functional recovery of Achilles tendon, which is promising to become a potential clinical treatment option.

1. Introduction

Achilles tendon rupture is a common sports injury, and the incidence is increasing year by year, due to sports popularity worldwide.[1] The annual incidence of Achilles tendon rupture is as high as 20 to 32 cases per 100000 people in Europe and the United States, mainly affecting young and middle-aged men. If not handled properly, Achilles tendon rupture can lead to a significant decrease in heel-lifting ability and gait changes, seriously affecting the patient's daily life and work. As a result, the importance of tendon repair research and clinical treatment is increasingly recognized and emphasized.

At present, tendon ruptures are mainly treated by surgical suture in the clinical practice, and let heal naturally in the later stage.[2] During this process, tendon adhesion becomes a common problem.[3] It is usually caused by exogenous healing, that is, the healing process involving external circulating cells from the adjacent tissues (such as paratenon and epitenon).[4] These cells can lead to excessive deposition of collagen matrix, causing tendon adhesion to surrounding tissues, which in further leads to limited joint mobility and pains. Strategies such as early functional exercises, drug therapy, and material barriers are employed to prevent tendon adhesions.[5] Early functional exercise is often difficult to implement due to the strict timing and poor patient compliance; drug therapy (such as glucocorticoids) may be accompanied by high costs and drug resistance. At present, scaffold and film based on macromolecular materials (e.g., polylactic acid, chitosan, cellulose, etc.) can be used as physical barriers to separate

R. Luo, Y. Xiong, J. Li, M. Xiao, Y. Bai, C. Li
Beijing Institute of Nanoenergy and Nanosystems
Chinese Academy of Sciences
Beijing 101400, China

Z. Li
Tsinghua Changgung Hospital
School of Clinical Medicine
Tsinghua University
Beijing 100084, China
E-mail: li_zhou@tsinghua.edu.cn

Z. Li
School of Biomedical Engineering
Tsinghua University
Beijing 100084, China

The ORCID identification number(s) for the author(s) of this article can be found under https://doi.org/10.1002/adma.202501306

DOI: 10.1002/adma.202501306

R. Luo, J. Li
School of Nanoscience and Engineering
University of Chinese Academy of Sciences
Beijing 100049, China

H. Feng
College of Materials Science and Opto-Electronic Technology
University of Chinese Academy of Sciences
Beijing 100049, China
E-mail: fenghongqing@ucas.ac.cn

C. Li, A. Liang
State Key Laboratory for Quality Ensurance and Sustainable Use of Dao-di Herbs
Institute of Chinese Materia Medica
China Academy of Chinese Medical Sciences
Beijing 100700, China

Z. Xu, Z. Luo
School of Material Science and Engineering
Tianjin University
Tianjing 300350, China

damaged tendons from surrounding connective tissues to avoid tendon adhesion.[6] In addition, by adjusting the surface structure of biomaterials to construct superhydrophobic surfaces, hydrophilic materials (form a hydrated layer), zwitterionic materials, etc., the deposition of collagen matrix can be further reduced while avoiding cell adhesion. However, these materials are usually prepared as scaffolds or films, which are difficult to adapt to the complex anatomical structure of the tendon.

Apart from the adhesion challenge, another problem related to tendon repair is insufficient endogenous healing that are completed by the stem cells inside the tendon.[7] Achieving endogenous healing is very difficult and often requires additional interventions.[8] Introducing exogenous stem cells through stem cell therapy and 3D printed multicellular scaffolds or recruiting endogenous stem cells through decellularized tendon slice can effectively promote endogenous repair of tendons, but these strategies face challenges of cell viability, tissue compliance, and high costs.[9] In addition, electrical stimulation generated by piezoelectric scaffolds comprised of aligned nanoscale fibers are reported to enhance endogenous healing by promoting the generation of tendon-like cells.[10] However, how to simultaneously promote endogenous healing and inhibit tissue adhesion caused by exogenous healing without interfering with each other is still an unsolved challenging problem.

In this study, we have developed a piezoelectric injectable anti-adhesive hydrogel (PE-IAH), which is designed to inhibit exogenous healing while promoting endogenous healing, in order to accelerate the functional recovery of injured tendon (**Figure 1**). The bioabsorbable natural materials carboxymethyl chitosan (CMCS) and hyaluronic acid (HA) are employed to form the injectable anti-adhesive hydrogel (IAH), which can effectively inhibit adhesion and inflammatory response both in vitro and in vivo. The piezoelectric property of the PE-IAH originates from annealed poly-L-lactic acid (PLLA) short nanofibers. PLLA is a biodegradable organic piezoelectric material with excellent biocompatibility and has been used as piezoelectric film and scaffolds in many studies.[11] PLLA is cut into short fibers and incorporated with the IAH to form a PE-IAH that can achieve both piezoelectric stimulation and anti-adhesion effect, while retaining the injectable properties of IAH. The PE-IAH can significantly promote the proliferation, differentiation and extracellular matrix remodeling of tendon stem cells/progenitor cells (TSPCs), and remarkably enhance the endogenous healing of tendon, both in vitro and in vivo. This works provides a simple and feasible strategy for rapid recovery of tendon function after rupture or tear.

2. Results and Discussion

2.1. Design and Characterization of the IAH

In clinical applications, sodium hyaluronate gel has been used to prevent adhesion after tendon surgery by providing lubrication.[12] However, the rapid absorption of sodium hyaluronate makes it difficult to form a long-lasting protective barrier at the injured tendon site.[13] Therefore, high molecular weight HA (MW: 200000-400000, 0.5%w/w), is used to replace sodium hyaluronate to get a slow absorption. CMCS is a water-soluble chitosan-derivate in which the hydroxyl groups in chitosan are replaced by carboxymethyl groups. CMCS has large number of —COOH groups, which will dissociate into negative groups at physiological pH (the isoelectric point of CMCS is 3–4) and form a repulsive force with the negative charges on the cell membrane, thereby preventing cells from adhering.[14] Direct mixing of CMCS and HA could not resist macrophage adhesion (Figure S1, Supporting Information). This may be due to the rapid diffusion of free CMCS and HA molecules into the liquid environment. Therefore, CMCS is cross-linked with genipin, a natural cross-linker derived from gardenia fruit. In the CMCS and HA mixed solution (PH>7.6), genipin reacts with the amino groups (—NH_2) in the CMCS to form a Schiff bond. HA is encapsulated in cross-linked CMCS (cCMCS) to form IAH (**Figure 2a**). Fourier transform infrared (FTIR) spectra showed that the characteristic peaks of CMCS were at 1653 cm^{-1} and 1598 cm^{-1}, representing stretching vibrations of —COO and C—O respectively. After CMCS was cross-linked with genipin, the characteristic peak 1598 cm^{-1} blue-shifted, and a new peak corresponding to the C-N bond appeared at 1031 cm^{-1} (Figure 2b; Figure S2, Supporting Information).

A series of IAH were prepared by adjusting the mass ratio of cCMCS to HA without changing the clinical therapeutic amount of HA (0.5% w/w) (Figure S3, Supporting Information). We aimed to make the hydrogel injectable so that they can easily be delivered to the injury site and wrap the Achilles tendon. As the mass ratio of cCMCS decreased, the IAH transitioned progressively from solid-like to liquid-like state (Figure S3, Supporting Information). IAH with cCMCS:HA = 1:2 and 1:3 was in liquid state, difficult to stay in the injured tendon sites. Therefore, only IAH with cCMCS:HA≥1:1 was chosen for further studies, and the dynamic rheological properties of them were investigated (Figure 2c,d). At a shear frequency of 1 Hz, the storage modulus (G′) of IAH is stably higher than the loss modulus (G″), confirming that IAH was in a gel state at the low frequency (Figure 2c). However, when the shear frequency of IAH was higher than 1 Hz, G′ suddenly decreased to be less than G″, indicating a transition of IAH from gel to sol state (Figure 2d). The higer cCMCS content, the higher shear force frequency required for the IAH to transform to sol state. Figure 2e showed the IAH with cCMCS:HA≥1:1 could be extruded from a syringe with an inner diameter of 0.33 mm, further demonstrating the shear-thinning properties and injectability of the IAH.

The anti-adhesion effects of those IAH were preliminarily verified by cell experiments. First, the cell counting kit-8 (CCK-8) test confirmed that IAH had no effect on the viability of fibroblasts, showing good biocompatibility (Figure S4, Supporting Information). Subsequently, IAH with different cCMCS:HA ratios were laid on half of the cell culture wells and co-cultured with macrophages and fibroblasts for 72 h (Figure 2f–h), because macrophages and fibroblasts are the key cells in the formation of adhesions after tendon injury.[15] The bright field microscopic images showed that in the groups with cCMCS:HA = 3:1, 2:1 and 1:1, fibroblasts had almost no adhesion to IAH, and a small number of macrophages adhered to the IAH. In the group with cCMCS:HA = 1:2, ≈15% of the IAH surface was covered by fibroblasts; and in the group with cCMCS:HA = 1:3, more fibroblasts adhered on the IAH surface (≈35%), and ≈10% of the IHA surface was covered by macrophages. This indicated that IAH with lower cCMCS ratio had poorer anti-adhesion ability. SEM

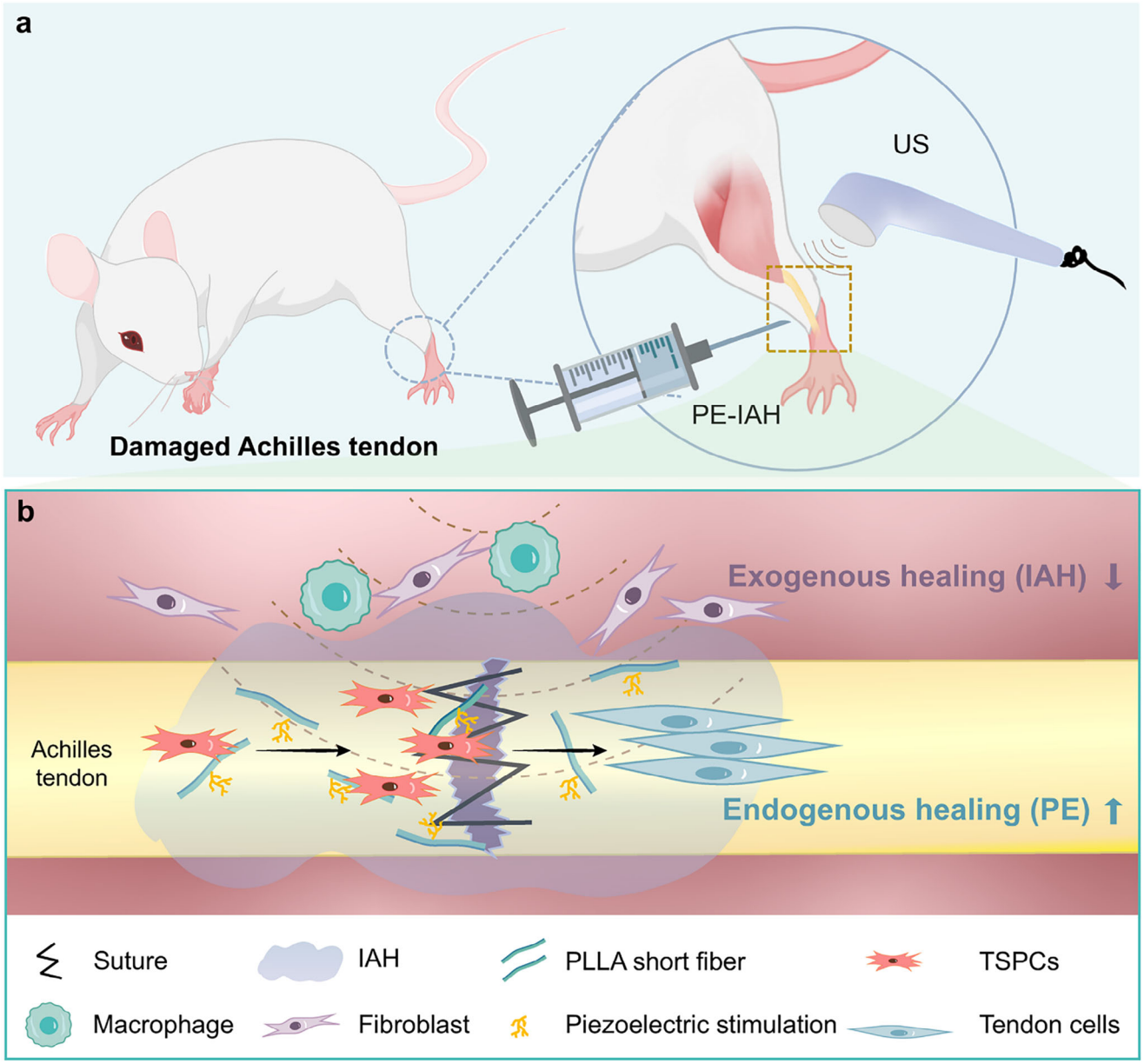

Figure 1. Schematic diagram of tendon treatment based on the PE-IAH. a) The PE-IAH injected into the injured tendon site is used in conjunction with ultrasound (US) to reduce tendon adhesion and promote endogenous tendon repair. b) The IAH acts as an anti-adhesion and anti-inflammatory physical barrier to prevent exogenous healing; while the incorporated PLLA short fibers in the IAH are driven by US to generate piezoelectric stimulation for promoting endogenous tendon repair.

images showed that as the content of cCMCS decreased, the porous structure (cCMCS matrix) on the surface of the IAH gradually became larger and disappeared, presenting a relatively flat plane (HA wrapping) (Figure S5, Supporting Information). We speculated that the low-content cCMCS matrix could not cover all areas due to the high diffusion of HA in the culture medium, which led to a reduced anti-adhesion ability of IAH.

M1 macrophages can produce a large number of proinflammatory cytokines and reactive oxygen species, including tumor necrosis factor-α (TNF-α), IL-1β, IL-12 and IL-23, which will recruit more proinflammatory cells.[16] M1 macrophages highly express nitric oxide synthase (iNOS) and produce NO, which can further aggravate inflammatory responses.[17] As the critical components of IAH, both cCMCS and HA have been shown to possess anti-inflammatory ability and can reduce the proportion of M1 macrophages.[18] Therefore, we co-cultured IAH with M1 macrophages induced by lipopolysaccharide (LPS) to observe the expression of iNOS in the M1 macrophages (Figure 2i; Figure S6, Supporting Information). Immunofluorescent images confirmed that compared with the Blank group, IAH could obviously downregulate the expression of iNOS, indicating that IAH retained the anti-inflammatory ability of cCMCS and HA.

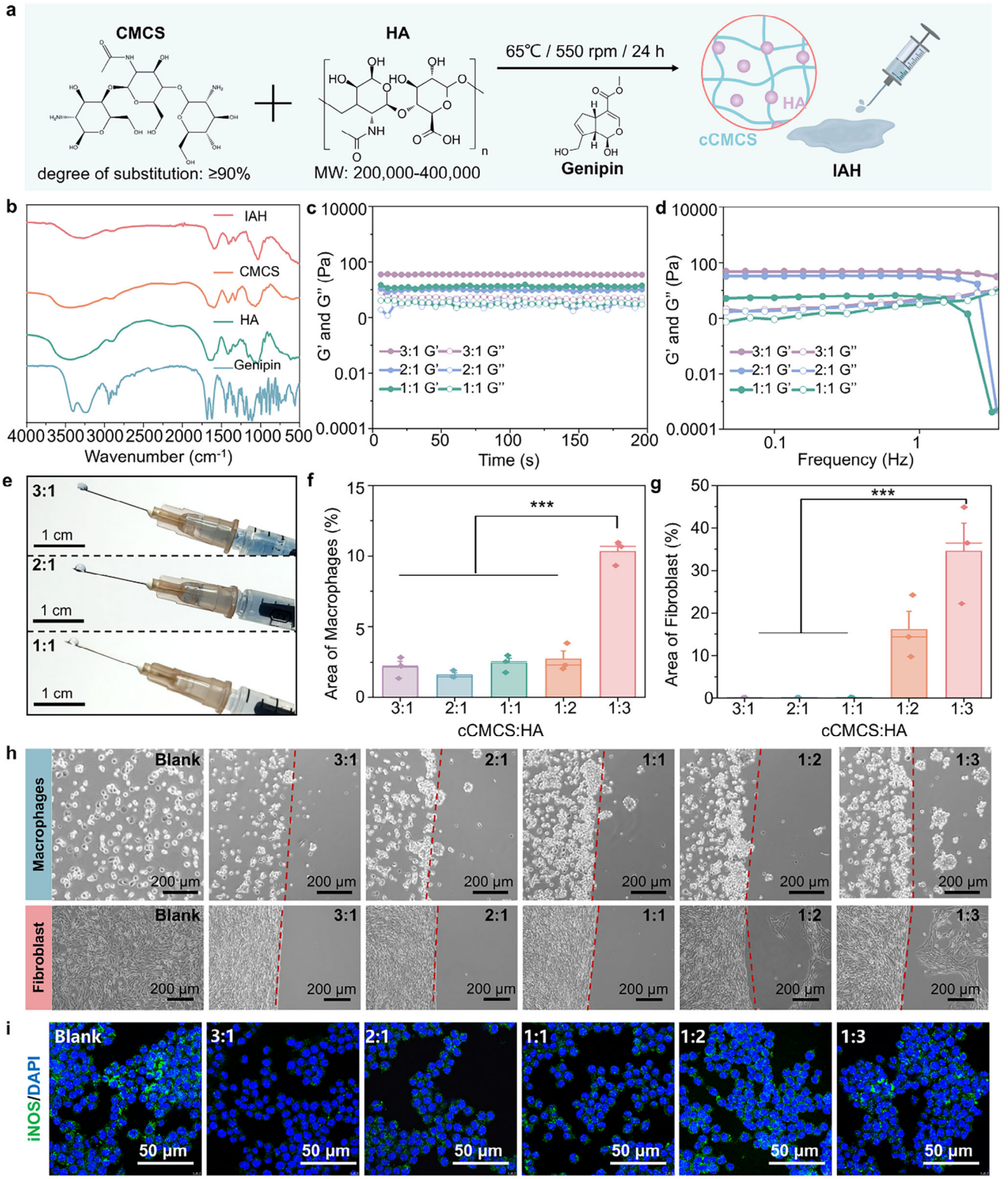

Figure 2. Preparation and characterization of the IAH. a) Fabrication process of the IAH. b) FT-IR of the IAH (cCMCS:HA = 1:1), CMCS, HA and genipin. Time sweep tests c) and frequency sweep tests d) of IAH with different cCMCS:HA ratios. e) Injectability of IAH with cCMCS:HA = 3:1, 2:1 and 1:1. The adhesion area of Raw 264.7 f) and NIH3T3 g) on the IAH with different cCMCS:HA ratios. h) Adhesion images of Raw 264.7 and NIH3T3 on the IAH with different cCMCS:HA ratios. i) Immunofluorescence images of iNOS expression in M1 macrophages after co-culture with IAH containing different cCMCS:HA ratios. f, g: $n = 3$ independent samples. *** $p < 0.001$. All statistical analyses were performed by one-way ANOVA, data are presented as mean ± S.E.M.

2.2. Design and Characterization of the PE-IAH

The PE-IAH was fabricated by incorporating piezoelectric PLLA short fibers into the IAH (**Figure 3**a). PLLA film was prepared by electrospinning, which showed piezoelectricity in the shear direction after annealing at 120 °C (Figure S7, Supporting Information). The high temperature causes the atomic arrangement of PLLA to shift, changing the polarity of the PLLA molecular chain and improving the crystallinity.[19] X-Ray Diffraction (XRD) spectra showed that PLLA had diffraction peaks on the (200) and (110) crystal planes, suggesting that it had piezoelectric property (Figure S7, Supporting Information). To further verify the electrical properties of PLLA, thin metal electrodes were attached on both sides of the PLLA film, and a voltage of about ±7 V was generated by finger tapping on the film (Figure S7, Supporting Information). The piezoelectric PLLA film was cut into short fibers with a length of 30 µm using a freezing microtome.[19] When the ratio of cCMCS:HA were = 3:1 and 2:1, PLLA short fibers were unable to distribute uniformly into the IAH. Taking into account the anti-adhesion, anti-inflammatory and injectability properties, the IAH with cCMCS:HA = 1:1 was selected to prepare the PE-IAH in subsequent studies. The concentration of PLLA in PE-IAH is the same as that in previous reports, which is 5 mg mL^{-1}[19] The PE-IAH were still injectable through a needle with a diameter of 0.33 mm (Figure 3b,c). The FTIR spectra confirmed that the stretching vibration peak of C = O of PLLA appeared at 1750 cm^{-1} in the PE-IAH (Figure S8, Supporting Information). SEM images revealed that PLLA short fibers were dispersed in the IAH (Figure 3d), because HA could act as a stabilizer to reduce the surface energy of the PLLA short fibers.[20] Considering that PE-IAH and IAH will be applied to Achilles tendon, we analyzed their mechanical stability by cyclic strain (1% or 1000%) (Figure 3e,f). PE-IAH and IAH turned into sol state (G′<G″) under large strain (1000%), and then recovered to gel state (G′>G″) when the strain was close to the static state (1%). These results indicated that PE-IAH and IAH could flow and recover under multiple pressures caused by tendon movement, and had tissue compliance ability.

We verified the piezoelectricity of the PE-IAH by XRD (Figure 3g), and the spectra showed that PE-IAH contained the amorphous carbon peak of the IAH and the crystalline peak of PLLA. The piezoelectric property of the PE-IAH was investigated by an oscilloscope under ultrasound (US) excitation (1 MHz, 0.5 W/cm^2, 50% duty cycle). The parameters of US are consistent with clinical applications, ensuring transdermal treatment while reducing thermal effects.[21] Due to the small size and inconsistent orientation of piezoelectric PLLA short fibers, it is difficult to distinguish the piezoelectric signal generated by them from the background noise caused by US (Figure 3h,j). Therefore, fast Fourier transform (FFT) was used to analyze the piezoelectric signals generated by PLLA short fibers. The FFT analysis showed that the major frequency of the piezoelectric signals were exactly 1 MHz (Figure 3i,k), suggesting that PLLA short fibers did have specific electric response to the US (Figure 3j,k). The IAH with piezoelectric PLLA short fibers (annealed) had a high peak at 1 MHz (Figure 3i), and the IAH with non-piezoelectric PLLA short fibers (unannealed) had a low peak at 1 MHz (Figure 3k). The IAH without PLLA short fibers had an low amplitude at 1 MHz that was similar to that of IAH with non-piezoelectric PLLA (Figure 3l), indicating that the low peak could be regarded as the background noise or triboelectric effect of IAH. This phenomenon confirmed that PE-IAH had good piezoelectric responsiveness under US excitation rather than triboelectric effect. After turning off US, the PE-IAH amplitude peak at 1 MHz disappeared (Figure 3m). The relationship between the amplitude generated at 1 MHz and the concentration of the piezoelectric fibers in the IAH was calibrated (Figure 3m,n; Figure S9, Supporting Information). Figure 3n confirmed that the amplitude gradually enhanced with the increase of PLLA short fiber content. These results confirmed that the PE-IAH could generate piezoelectric stimulation under US excitation.

The biocompatibility and anti-adhesion property of the PE-IAH were also investigated. The co-culture experiments involving NIH3T3 with the PE-IAH and its single components confirmed that PE-IAH was non-cytotoxic, and had no effect on the normal cell proliferation (Figure S10, Supporting Information). In addition, the PE-IAH did not cause hemolysis (<5%) after co-culture with red blood cells, thereby further validating the biocompatibility of the PE-IAH (Figure S11, Supporting Information). The anti-adhesion experiment of PE-IAH was conducted using fibroblasts and macrophages. (Figure S12, Supporting Information). The cell adhesion was not observed in the group containing the IAH, which showed the anti-adhesion effect came from the IAH solely, but not US and piezoelectric stimulation. Moreover, platelets extended pseudopodia and adhered extensively to the surface of PLLA short fiber, whereas less to the PE-IAH and IAH, adopting a disc-like shape without pseudopodia (Figure S13, Supporting Information). The above results proved that the PE-IAH had both excellent biocompatibility and anti-adhesion properties as same as the IAH.

2.3. Anti-Inflammatory Effects and Promotion of TSPCs of the PE-IAH In Vitro

To promote tendon healing, anti-inflammatory approaches are also important apart from the anti-adhesion approaches, because the activation of M1 macrophages and the sustained expression of their proinflammatory cytokines can cause chronic inflammation, further leading to tendon adhesion.[15] Therefore, the anti-inflammatory properties of the PE-IAH were also investigated. Considering that the acidic degradation products of PE-IAH may change the pH and aggravate the inflammatory response,[22] it is necessary to detect the pH of PE-IAH during the degradation process. Figure S14 (Supporting Information) showed that the pH in the PE-IAH group did not fluctuate significantly during the 15-day monitoring. iNOS is a chronic inflammatory marker expressed by M1 macrophages, and its expression level is used to assess the severity of the inflammatory response. **Figure 4**a,b showed that the iNOS expression in the PE group (PLLA + US, no IAH) were the same level as the Blank goup, suggesting that bare piezoelectric stimulation had no effect on the inflammatory response of the macrophages. Meanwhile, the iNOS expression in the IAH and PE-IAH groups were both significantly lower than the Blank and PE group. More anti-inflammatory results were shown in Figure S15 (Supporting Information). These results demonstrated the anti-inflammatory effect of the PE-IAH was as

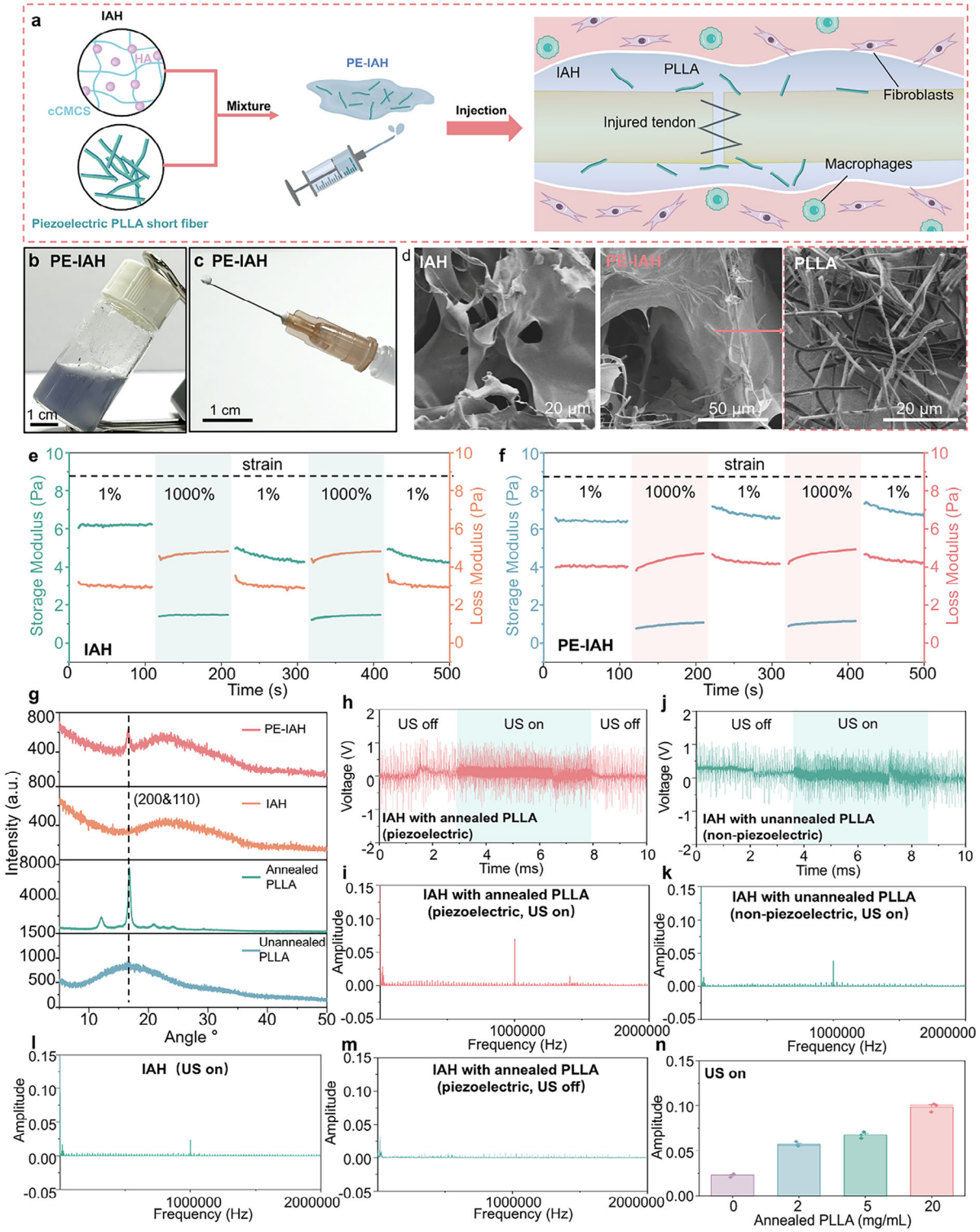

Figure 3. Preparation and characterization of the PE-IAH. a) Schematic diagram of the preparation of the PE-IAH and its wrapping around the injured tendon. b) Liquidity of the PE-IAH. c) Injectability of the PE-IAH (needle inner diameter: 0.33 mm). d) SEM images of PE-IAH, IAH and PLLA short fibers. e,f) The alternate step strain sweep test of the IAH (e) and PE-IAH (f). g) XRD spectra of PE-IAH, IAH, annealed PLLA and unannealed PLLA. h,i.) The voltage of IAH with 5 mg mL^{-1} annealed PLLA (piezoelectric) excited by US (1 MHz) (h) and the frequency spectrum obtained by the FFT (i). j, k) The voltage of IAH with 5 mg mL^{-1} unannealed PLLA (non-piezoelectric) excited by US (1 MHz) (j) and the frequency spectrum obtained by the FFT k). l. Frequency spectra of IAH (0 mg mL^{-1} PLLA) with US (1 MHz) analyzed by FFT. m. Frequency spectra of IAH without US analyzed by the FFT. n. Amplitude at 1 MHz extracted from the frequency spectra with different concentration of the piezoelectric fibers. n: $n = 3$ independent samples. All statistical analyses were performed by one-way ANOVA, data are presented as mean ± S.E.M.

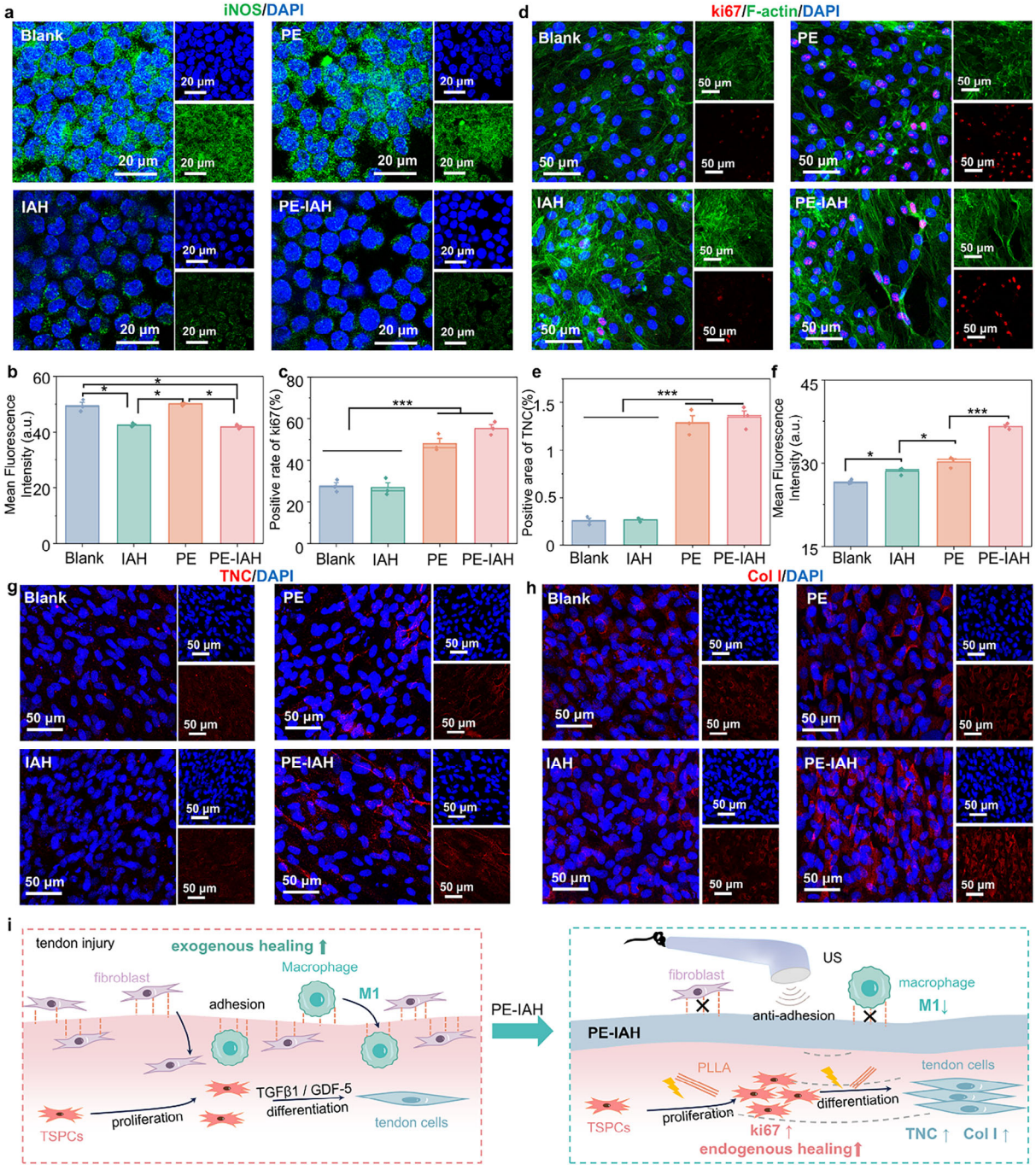

Figure 4. Effects of the PE-IAH on the key cells involved in tendon adhesion and repair in vitro. a) Immunofluorescence staining images of iNOS in the M1 macrophages. b) Mean fluorescence intensity of iNOS in the M1 macrophages. c). Positive rate of ki67 in the TSPCs. d). Immunofluorescence staining images of ki67 in the TSPCs. e). Positive area of TNC in the TSPCs. f). Mean fluorescence intensity of Col I in the TSPCs. g). Immunofluorescence staining images of TNC in the TSPCs. h). Immunofluorescence staining images of Col I in the TSPCs. i). Schematic diagram of the effects of PE-IAH on cells. b, c, e f: $n = 3$ independent samples. * $p < 0.05$ and *** $p < 0.001$. All statistical analyses were performed by one-way ANOVA, data are presented as mean ± S.E.M.

satisfactory as the IAH, without being affected by the piezoelectric stimulation.

Apart from anti-adhesion and anti-inflammation, tendon regeneration, or in other words, endogenous healing, is particularly important during the repair of tendon injury.[23] In this process, endogenous tenocytes synthesize and secrete new extracellular matrix such as collagen to fill the damaged area. However, due to the limited tenocytes proliferation, endogenous healing of tendon usually depends on tendon stem cell proliferation and tenogenic differentiation.[24] The effects of PE-IAH on TSPCs

(coming from Achilles tendon) proliferation and differentiation are investigated in vitro (Figure 4c,d; Figure S16, Supporting Information). The images showed that the positive rate of ki67 in the IAH group (≈26.9%) and PLLA-IAH group (≈31.0%) was not significantly different from the Blank group (≈27.6%), indicating that the IAH had no ability to promote the TSPCs proliferation. The ki67 positive rate of the TSPCs in the US group (≈36.7%) and US-IAH group (≈39.6%) was significantly increased (Figure S16, Supporting Information), and the rate was further enhanced in the PE group (PLLA + US, no IAH) to ≈48.1% (PE group). The rate of the TSPCs in the PE-IAH group (≈55.3%) was slightly higher than the PE group, but there was no statistical difference ($p = 0.1533$) (Figure 4c). These results indicated that bare IAH was not able to promote TSPCs proliferation, but the PE was able to play the role; when the PE was incorporated with the IAH, the promotion ability of the PE was not impaired, but even a little enhanced in the PE-IAH.

The effect of the PE-IAH on the tenogenic differentiation of the TSPCs was researched in vitro (Figure 4e,h; Figure S17, Supporting Information). Tenascin C (TNC) is expressed during the development and maturation of tendon tissue, and is considered an important marker of tenocyte differentiation.[25] Compared with the Blank group (≈0.25%), the TNC expression in the TSPCs of the IAH group (≈0.26%), PLLA-IAH group (≈0.24%), US-IAH group (≈0.44%) and the US group (≈0.41%) was not significantly upregulated, while the PE group (≈1.28%) and PE-IAH group (≈1.32%) increased by ≈3 times (Figure 4e,g; Figure S17, Supporting Information). This indicated that PE could promote tenogenic differentiation, which was specific and almost unaffected by the bare IAH, PLLA and US. Col I is an extracellular matrix secreted by the TSPCs and tenocytes, and especially in large quantities when the TSPCs differentiate into tenocytes.[26] Compared with PE group (≈30.2%), the the secretion of Col I increased by ≈21.2% in the PE-IAH group (≈36.6%), which was an additional benefit, different from the TNC expression (Figure 4f,h; Figure S17, Supporting Information). The reason might be that CD44, as a membrane receptor for HA, is expressed in abundance in the TSPCs, and the HA in the IAH promotes cell secretion of collagen after binding to it.[18]

In conclusion, the PE-IAH was demonstrated to reduce the expression of iNOS in the M1 macrophages due to the IAH, thereby achieving anti-inflammatory effects. Besides, it promoted the proliferation, differentiation and extracellular matrix remodeling of the TSPCs through the piezoelectric responses of PLLA short fibers to US in the IAH. This confirmed that the PE-IAH had the potential to inhibit exogenous tendon healing and promote endogenous healing in vivo (Figure 4i).

2.4. Inhibition of Exogenous Healing by the PE-IAH After Tendon Injury In Vivo

First of all, the in vivo biocompatibility of the PE-IAH was evaluation, PLLA, IAH and PE-IAH were injected subcutaneously in rats. After 28 days, pathological sections of the main organs were performed and found to be the same as normal rats. There was no edema or abnormal inflammatory cell infiltration, which showed that all materials had good biocompatibility in vivo (Figure S18, Supporting Information). In addition, lead zirconate titanate (PZT) was implanted into the abdominal cavity of rats as a sensor, and US was applied to the skin. A peak at 1 MHz was observed in the frequency spectra analyzed by FFT, ensuring that that US could penetrate the skin and drive the piezoelectric materials to generate piezoelectric output (Figure S19, Supporting Information). For ruptured tendons, a suture method with strong tensile strength is often used in clinical practice.[27] Therefore, rats with ruptured Achilles tendons sutured by modified Kessler suture were made as the animal model (Figure S20, Supporting Information). Sutured Achilles tendons of rats in the Blank group received no treatment, and the other groups were injected with IAH or others, with or without US. The treatment groups involved in this study included: IAH group, PE-IAH group (PLLA short fibers + IAH, with US), PLLA-IAH group (PLLA short fibers + IAH, no US), and PE group (PLLA short fibers+1×PBS, with US). The US (0.5 W/cm^2, 50% duty cycle) was applied for 20 min day^{-1} in 2-days-US and 1-day-rest pattern (**Figure 5a**).

On the 8th day, the Achilles tendons of rats in different groups were exposed. The results showed that the Achilles tendons injected with IAH (IAH group, PLLA-IAH group and PE-IAH group) were all easy to separate and had a clear boundary with the surrounding tissues, while in the Blank group the tendon was closely adhered to the surrounding tissue (Figure 5b). In addition, we found that the tendon tissue in the PE group had not only tissue adhesion, but also discontinuous structure. The adhesion of the rat Achilles tendon was further observed by Masson staining. As shown in Figure 5c, dense collagen fibers were formed near the tendons in the Blank and PE groups, while the presence of the IAH reduced the adhesion of injured tendon, which was manifested as sparse arrangement of collagen fibers around the tendon. Subsequently, we observed the long-term effects of the PE-IAH on tendon repair. On the 14th day and 28th day after surgery, there was almost no adhesion between the injured tendon and the surrounding tissue in the PE-IAH group, which meant that the anti-adhesion effect of PE-IAH was sustained. (Figure S21, Supporting Information).

Injury-related inflammatory responses and cytokines induce the recruitment of fibroblasts and inflammatory cells to the injury site to proliferate and secrete collagen, leading to exogenous repair of the tendon.[15,28] Neutrophils are the first inflammatory cells to be recruited in the early stage of inflammation, followed by a large number of mononuclear macrophages being recruited to the lesion.[29] H&E (hematoxylin-eosin) staining of tendon tissue on the 3rd day was performed (Figure 5d,e). Pathological images showed that the density of inflammatory cells in the PE group (≈289 pieces/0.2 mm^2) was slightly higher the Blank group (≈235 pieces/0.2 mm^2), which probably because the acidic degradation byproducts of PLLA had induced some local inflammatory response.[30] The density of inflammatory cells in the PE-IAH group (≈51 pieces/0.2 mm^2) and PLLA-IAH group (≈51 pieces/0.2 mm^2), being similar to the IAH group (≈61 pieces/0.2 mm^2), was significantly lower than the PE group ($p<0.001$), indicating that the presence of the IAH was conducive to the resolution of acute inflammation in the injured tendon, and its dispersion effect on PLLA alleviated or even eliminated the local inflammatory response caused by PLLA degradation.

The HE staining images showed many inflammatory cells including a large number of macrophages on the 3rd day (Figure 5d). High amount of M2a macrophages will promote

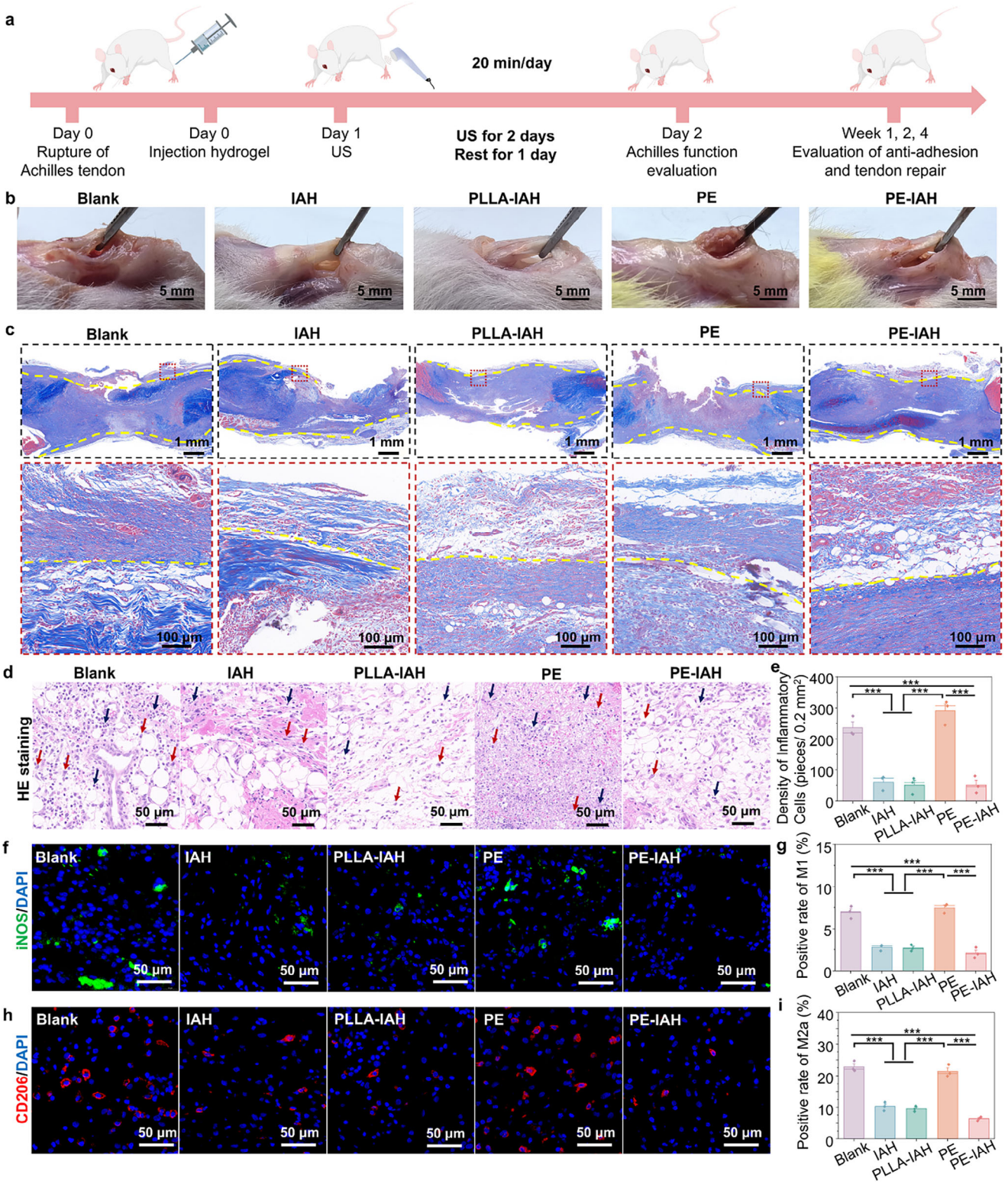

Figure 5. Effects of the PE-IAH on tendon adhesion and inflammatory response in rats. a) Timeline of treatment for ruptured Achilles tendon using the PE-IAH. b) Achilles tendon images on the 8th day. c) Masson staining of Achilles tendon on the 8th day. d) H&E staining of Achilles tendon on the 3rd day. Black arrows: Neutrophils; Red arrows: macrophages. e) Density of inflammatory cells. f) Immunofluorescence staining images of iNOS in the Achilles tendon on the 3rd day. g) Positive rate of M1 macrophages. h) Immunofluorescence staining images of CD206 in the Achilles tendon on the 3rd day. i) Positive rate of M2a macrophages. e, g, i: $n = 3$ independent samples. *** $p < 0.001$. All statistical analyses were performed by one-way ANOVA, data are presented as mean ± S.E.M.

fibroblasts to secrete a large amount of collagen and fibrosis.[31] Therefore, we used specific markers to indicate different types of macrophages: M1 macrophages were marked by iNOS, and their content represents the level of tissue inflammation; M2a macrophages were marked by CD206, which are correlated with tissue adhesion and fibrosis.[32] The results showed that the infiltration of M1 and M2a macrophages in the Achilles tendon tissue treated with the PE-IAH was decreased to ≈2.1% and ≈6.4%, respectively, while the PE group (7.5%, and 21.4%, respectively) showed no difference compared with the Blank group (7.0% and 22.8%, respectively) (Figure 5f–i). These evidences further suggested that the PE-IAH could reduce the infiltration of tissue inflammation and the formation of fibrosis, which was beneficial to inhibit tissue adhesion after tendon injury. Consistent with the results of the cell experiment, the inhibition of exogenous repair of the PE-IAH was mainly caused by the IAH, which was not interfered by the incorporation of PLLA short fiber and US application. The PE-IAH group successfully improved the immune microenvironment of tendon regeneration as a physical barrier and inhibited fibrosis caused by exogenous healing.

2.5. Promotion of Endogenous Healing by the PE-IAH After Tendon Injury In Vivo

The endogenous healing is a critical period for tendon repair.[33] During this stage, tenocytes and tendon stem cells are activated to form new tendon tissue through proliferation, differentiation, and collagen secretion, thereby reconnecting the ruptured tendon fibers. The structure and integrity of the proliferative tendon in each group was examined by HE staining. The Achilles tendon tissue images on the 8th day showed that the PE-IAH group had a complete and neat new tendon structure. Conversely, the IAH group, PLLA-IAH group and PE group all had large defects, especially the PE group, where a large number of PLLA short fibers were present in the new tendon tissue (**Figure 6a**). However, there were almost no PLLA short fibers in the new tendon tissue of the PLLA-IAH group and the PE-IAH group. The PLLA short fibers were only found in the loose connective tissue around the tendon, which indicated that the PLLA short fibers were effectively incorporated in the IAH, and the PE-IAH could ensure the integrity of the regenerated tendon. The long-term evaluation of tendon repair quality was further performed. Pathological images of the tendon rupture site on the 14th and 28th day showed that PE-IAH had the best therapeutic effect, showing tightly arranged tendon tissue. In particular, on the 28th day, the tendon fibers in the PE-IAH group were neatly arranged, while the US-IAH and PLLA-IAH groups were disordered (Figure S22, Supporting Information). In addition, we also paid attention to the degradation of PLLA in vivo (Figure S23, Supporting Information). The images of pathological sections showed that a small amount of PLLA short fibers in the PE-IAH group were in the form of clumps on the 14th day, while more were found in the PE group; We speculated that IAH dispersed the PLLA short fibers evenly, and then the PLLA short fibers with relatively small size are more easily degraded under US.[34] The phenomenon that the size of PLLA gradually shortened during the degradation process was clearly observed in the in vitro degradation experiment (Figure S14, Supporting Information).

For further verification, the expression of proteins related to the proliferation and differentiation of TSPCs in the Achilles tendon tissue were detected on the 8th day. Immunofluorescence staining images showed that the tendon tissue exhibited certain amount of ki67 positive cells in the repair period (Figure 6b,c). Compared with the Blank group, PLLA-IAH group and the PE group all significantly increased the positive rate of ki67, which was 1.83 times and 2.17 times that of the Blank group, respectively, indicating that a large number of cells were in mitosis. This finding was consistent with the results of the cell experiment, that is, the PE could promote cell proliferation; both IAH and PE played coordinated roles in the PE-IAH group, further increasing the proportion of ki67-positive cells (≈22.9%). In addition, TNC was also expressed abundantly in the new tendon tissue of the PE-IAH group (≈17.1%), which was significantly higher than the PLLA-IAH group (≈8.5%), suggesting that it was the piezoelectric effect but not bare PLLA in the IAH that played the role of promotion (Figure 6d,e). Meanwhile, unlike the results of the cell experiment, the expression of TNC in the PE group (≈7.6%) was notably lower than the PE-IAH group. These results indicated that it was difficult for the PE alone to promote the differentiation of TSPCs in vivo, which might be due to lacking regulation of the repair microenvironment by the IAH. As an important component in the new tendon tissue (Figure 6f,g), the content of Col I in the PE-IAH group was ≈6 times higher than the Blank group. The Col I content in the IAH group (≈10.6%), PLLA-IAH group (12.5%), and PE group (≈14.3%) was only 30.3%, ≈36.1%, and 41.7% of that in the PE-IAH group (≈34.7%), respectively. In addition, the Col I in the PE-IAH group were more directional than the other groups, which was important for tendon healing and functional recovery. The above outcome verified that the piezoelectric stimulation generated by PLLA short fibers in combination of IAH in the PE-IAH group could achieve overwhelming endogenous repair of the tendon, ultimately ensuring the regeneration of the complete tendon structure.

The recovery of tendon function is the key to evaluating the effectiveness of the treatment method. Paw prints were collected on the 2nd day, 8th day and 14th day after modeling (Figure 6h; Figure S24, Supporting Information), and the Achilles Functional Index (AFI) was obtained by analyzing the gait of rats.[35] The results on the 2nd day showed that the AFI of rats in the IAH group (−92.0) and PLLA-IAH group (−88.4) were significantly higher than the Blank group (−105.9) and the PE group (−104.2), indicating that the IAH was advantageous to the early recovery of Achilles tendon function. More importantly, in the PE-IAH group, the AFI of −60.6 demonstrated the strong synergistic effect of the piezoelectric stimulation and the IAH. This result suggested that PE together with anti-adhesion approach was much more advanced than bare anti-adhesion approaches in promoting tendon function recovery. If PE was applied without the IAH (PE group), the tendon would suffer from structural discontinuity and severe adhesion, leading to poor functional recovery. The gait analysis results on the 8th day had a consistent trend with that on the 2nd day. In addition, the AFI of rats in the US-IAH group was close to the IAH group during the 2-week observation period, which confirmed that US had no significant effect on promoting the recovery of rat Achilles tendon function (Figure S24, Supporting Information). On the 14th day, the Achilles tendon function

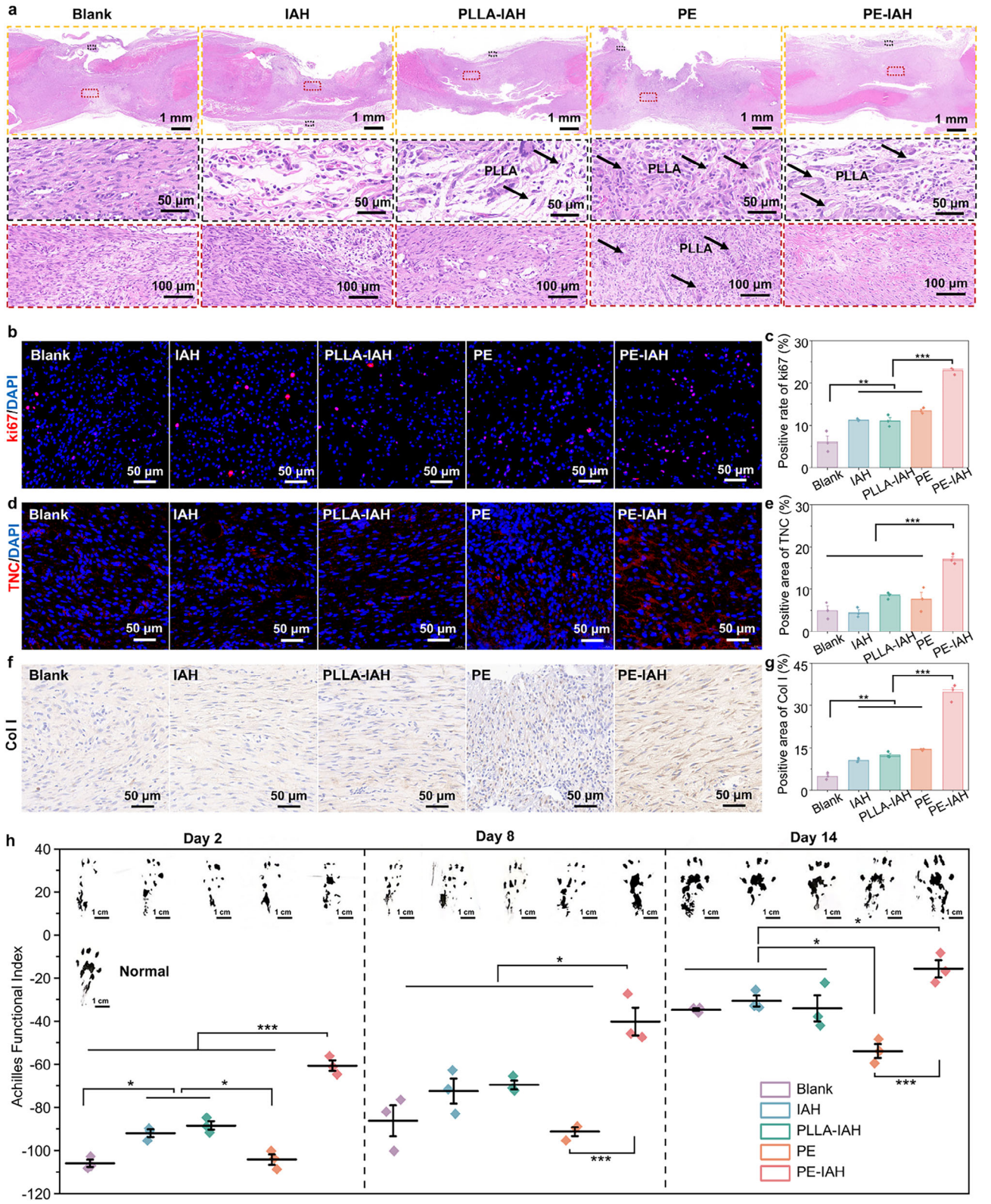

Figure 6. Effects of the PE-IAH on tendon repair and function recovery. a) H&E staining of Achilles tendon on the 8th day. Black arrows: PLLA short fibers. b) Immunofluorescence staining images of ki67 in the Achilles tendon on the 8th day. c) Positive rate of ki67. d) Immunofluorescence staining images of TNC in the Achilles tendon on the 8th day. e) Positive area of TNC. f) Immunohistochemical images of Col I in the Achilles tendon on the 8th day. g) Positive area of Col I. h) Paw prints (injury and normal) and Achilles Functional Index of rats on the 8th day. c, e, g, h: $n = 3$ independent samples. * $p < 0.05$, ** $p < 0.01$ and *** $p < 0.001$. All statistical analyses were performed by one-way ANOVA, data are presented as mean ± S.E.M.

index of PE-IAH could be restored to a near normal level (−15.6), which is ∼50% that of the IAH group (−30.6).

In general, the PE-IAH could promote endogenous healing after tendon injury. Particularly, the IAH served as an effective anti-adhesion barrier and provided favorable immune microenvironment, and the piezoelectric stimulation generated by US-excited PLLA short fibers promoted the proliferation and differentiation of tendon stem cells. The synthetic effects of PE and IAH achieved perfect repair of the Achilles tendon and promoted the functional recovery of the injured Achilles tendon.

3. Conclusion

In summary, we developed a fully degradable piezoelectric injectable anti-adhesive hydrogel (PE-IAH) based on the mechanism of tendon endogenous healing. The PE-IAH retained the good mechanical stability and shear-thinning properties, and could be injected to wrap the injured tendon. The physical barrier and anti-inflammatory effect of the IAH reduced the exogenous healing from the tissue around the tendon, providing suitable immune microenvironment for the tendon endogenous healing. The piezoelectric PLLA short fibers in the PE-IAH could generate piezoelectric stimulation under US excitation, which were demonstrated to promote the proliferation and differentiation of endogenous TSPCs into tenocytes, and rebuilt the extracellular matrix through the synthesis and secretion of collagen. In addition to promoting tendon healing, the synergistic effect of piezoelectric stimulation and the IAH also greatly reshaped the biomechanical function of the tendon and restored the movement function of rats with tendon rupture. This strategy provides a more efficient and safer new method for clinical treatment, which is expected to improve the rehabilitation effect and life quality of patients with tendon injuries.

4. Experimental Section

Preparation and Characterization of the IAH: CMCS (Macklin, C902396, degree of substitution: ≥90%) was prepared into 0.33% w/w, 0.5% w/w, 1% w/w, 2% w/w, and 3% w/w aqueous solutions with phosphate buffered solution (1×PBS). 1% w/w aqueous solution of HA (Macklin, H909936, MW: 200000∼400000) was prepared in the same way. CMCS solutions of different concentrations were mixed with 1% w/w HA solution in equal volumes, and then the IAH with different proportions was prepared by cross-linking with 1% w/w genipin at 65 °C for 24 h and stirring at 500 rpm. The injectability of the IAH was evaluated using a 1 mL syringe (needle inner diameter 0.33 mm). Fourier transform infrared spectrometry (FT-IR, VERTEX80v, Bruker) was used to demonstrate that CMCS had been successfully cross-linked. The surface morphology of the IAH was observed using a cold field emission scanning electron microscope (SEM, SU8020).

Preparation and Characterization of PLLA Fiber Film: Piezoelectric PLLA fibers were prepared using an electrospinning machine.[19] 1 g PLLA (PLLA004, Esunmed, intrinsic viscosity: 1.2-1.5 dL g^{-1}) was dissolved in 5 mL hexafluoroisopropanol solution and stirred at room temperature for 2 h until PLLA was completely dissolved to obtain a uniform spinning solution. The above solution was added to a syringe, and the syringe was mounted on a syringe pump. The polymer solution flow rate was set at 1 mL h^{-1}, the time was set to 40 min, flowed through a G22 needle, a positive voltage of 12 kV was applied, and collected on a roller covered with aluminum foil at 2500 rpm to obtain an aligned nanofiber mat. A negative voltage of -2 kV was applied to the roller, and the relative humidity was controlled at 30±10%. The PLLA nanofiber film was annealed at 120 °C for 8 h and slowly cooled to room temperature to obtain the annealed PLLA. X-ray Powder diffractometer (XRD, Xpert3 Powder) was used to observe the crystallinity of PLLA, and SEM (SU8020) was used to evaluate the directionality of PLLA. The piezoelectric response of PLLA after annealing was measured using an oscilloscope (Teledyne LeCroy HD 4096). Electrodes were attached to the front and back sides of the PLLA film and connected to an oscilloscope through a wire, and the voltage was measured during the entire process.

Preparation and Characterization of PLLA Piezoelectric Short Fibers: The annealed PLLA film was embedded with a cryoembedding agent (4583, SAKURA), cut into short fibers (30 µm) using a freezing microtome (CM3050S, Leica), washed with deionized water, and freeze-dried to obtain PLLA short fibers. The morphology and size of the PLLA short fibers were observed using SEM.

Preparation and Characterization of the PE-IAH: Equal volumes of 1% w/w CMCS solution, 1% w/w HA solution, and 5 mg mL^{-1} of annealed PLLA short fibers were stirred at 500 rpm at room temperature for 2 h. Following the same method used for synthesizing the IAH, 1% w/w genipin was added to the mixture containing PLLA short fibers for cross-linking reaction to prepare the PE-IAH. The injectability and surface morphology were the same as the characterization method of the IAH. The PE-IAH prepared using PLLA of different masses was incorporated into the IAH, electrodes were attached to the front and back sides, and the PE-IAH was driven by an ultrasonic physiotherapy device (27335, Chattanooga) and the voltage signal was measured by an oscilloscope. The frequency of the ultrasonic physiotherapy device was 1 MHz, the power was 0.5 W cm^{-2}, and the duty cycle was 50%. The penetration ability of ultrasound was calibrated by using PZT as a piezoelectric transducer.

The degradation of PE-IAH (200 µL/well) was carried out in 1 mL Simulated Body Fluid (SBF, Solarbio, G0390), which contained ∼400 UI/mL of hyaluronidase (YUANYE, S10060). The samples were incubated in shaking incubators, the temperature was set to 37 °C, and the rotation frequency was 60 times/min. The pH of SBF was tested on the Day 0, 1, 2, 3, 5, 7, 9, 11, and 13, and the images of PLLA short fibers were taken using a microscope on Day 1 and Day 14.

Rheological Behaviors: Rheological properties of IAH and PE-IAH were performed using an MCR 302 rheometer (Anton-Paar, Austria) at 25 °C. The gap in the parallel-plate rheometer was 1 mm. Frequency sweep tests were performed at 1% strain with a frequency range of 0.1–100 Hz. Time sweep tests were performed at 1% strain with a frequency of 1 Hz and a time range of 0–180 s. The alternate step strain sweep test of the IAH and PE-IAH was performed at a fixed frequency of 1 Hz, with strain values switching from 1% (small strain, 0.05 Pa) to 1000% (large strain, 50 Pa), with each strain interval lasting 100 s. During the measurements, both the storage modulus (G′) and the loss modulus (G″) were recorded.

Hemolysis Test and Platelet Adhesion Test: Hemolysis test and platelet adhesion test were approved by the University Animal Resources Committee (2023031LZ). 2 mL of fresh blood was collected from 6-week-old male SD rats. The blood was placed in a centrifuge tube for 30 min and centrifuged at 1000 rpm for 10 min to separate the blood. The white film between the red blood cells and the serum was taken as platelets. 2 µL of platelets were placed on the surface of 100 mg PLLA (5 mg mL^{-1} in 1×PBS), IAH and PE-IAH (5 mg mL^{-1} PLLA), and incubated at 37 °C for 90 min. All materials were sterilized by pasteurization, that was, boiling in the water bath at 65 °C for 30 min. After being fixed with 4% paraformaldehyde (Solarbio, P1110) for 30 min, they were dehydrated in different concentration gradients of ethanol (25%, 40%, 50%, 60%, 70%, 80%, 90%, 95%, and 100%) for 30 min. After evaporating to dryness at room temperature, the morphology of platelets on the surface of the material was observed by SEM (SU8020). The remaining blood was washed with PBS (1×, Solarbio, P1020) for 5 times and resuspended in 10 mL1× PBS. 0.2 mL of resuspended red blood cells were mixed with 0.8 mL of working solution, incubated for 4 h, centrifuged at 1000 rpm for 5 min in a centrifuge, and photographed and recorded. Take the supernatant and measure the OD value (541 nm) with an enzyme-labeled instrument.

$$\%\ \text{hemolysis} = \left(OD_{test} - OD_{neg}\right) / \left(OD_{pos} - OD_{neg}\right) \times 100\% \quad (1)$$

Working solution: positive group: 0.3% Triton X-100 (Solarbio, T8200); negative group: PBS (1×); material group: 1 mg material + PBS (1×)

Cell Culture: NIH3T3 and Raw 264.7 were obtained from the Cell Bank of the Chinese Academy of Sciences (Beijing). NIH3T3 and Raw 264.7 were cultured in high-glucose DMEM medium (11 995, Solarbio) containing 10% fetal bovine serum (FBS, Gibco) and 1% penicillin/streptomycin (P1400, Solarbio). Cell culture conditions were a humidified incubator (CCL-170B-8, ESCO) at 37 °C with 5% CO_2.

Raw 264.7 was induced with complete medium containing 100 ng mL^{-1} LPS (00-4976-93, Thermo Fisher) for 24 h to obtain M1 macrophages. TSPCs were derived from the Achilles tendons of 6-week-old male rats.[36] TSPCs were replicated less than 8 times to ensure their stem cell activity. Tenogenic differentiation of TSPCs required the addition of 0.05 mM L-Ascorbic acid 2-phosphate (HY-103701, MedChemExpress), 10 ng mL^{-1} GDF-5 (HYP72633, MedChemExpress), and 10 ng mL^{-1} TGF-β (HY-P70648, MedChemExpress).

Biocompatibility in Vitro: NIH3T3 was co-cultured with 10 mg of IAH and PE-IAH in different ratios in 96-well plates for 24 h, 48 h, and 72 h. Cell Counting Kit-8 (CCK-8, CA1210, Solarbio) and the Live/Dead Cell Double Stain Kit (CA1630, Solarbio) were used to detect cell viability. The absorbance of the supernatant after the reaction of CCK-8 and cells was measured using a microplate reader (BioRad iMark) at a wavelength of 450 nm. A confocal fluorescence microscope (Leica SP8) was used to take pictures of live and dead cells of NIH3T3.

Cell Adhesion Assays: IAH or PE-IAH was applied to one side of the wells of a 24-well plate, and sterilized in a UV light (265 nm). Raw 264.7 and NIH3T3 were plated at 1×10^5 for 48 h, and images were taken by a bright field microscope.

Expression Assay of M1 Macrophages: M1 macrophages were co-cultured with 100 mg IAH with different amounts of CMCS for 48 h to evaluate the anti-inflammatory effect of IAH. The PE-IAH anti-inflammatory effect experiment was divided into Blank group (no intervention), IAH group (100 mg IAH), PLLA group (0.2 mg mL^{-1} PLLA), PLLA-IAH group (100 mg IAH and 0.2 mg mL^{-1} PLLA), US group (2 min day^{-1} US for 2 days), US-IAH group (100 mg IAH + 2 min day^{-1} US for 2 days), PE group (0.2 mg mL^{-1} PLLA + 2 min day^{-1} US for 2 days), and PE-IAH group (100 mg IAH and 0.2 mg mL^{-1} PLLA + 2 min day^{-1} US for 2 days). The frequency of US was 1 MHz, the power was 0.5 W cm^{-2}, and the duty cycle was 50%. PLLA short fibers were sterilized by soaking in 75% ethanol (1 day), and PE-IAH and IAH were sterilized by pasteurization. Immunofluorescence staining was used to detect the expression of iNOS.

Proliferation and Differentiation of TPSCs: 1×10^5 TPSCs were placed in each well of a 48-well plate for 24 h. The proliferation assay of TPSCs was performed for 2 days, and the differentiation assay was performed for 1 week. The experimental groups were the same as those in the "Expression assay of M1 macrophages". Immunofluorescence staining was used to detect the expression of ki67, TNC, and Col I.

Immunofluorescence Staining of Cells: After fixation with 4% paraformaldehyde (Solarbio, P1110) for 15 min, the cells were washed three times with 1×PBS. Cells were blocked with 3% BSA (SW3015, Solarbio) and 10% FBS (10099-141, Gibco) in 0.5% Triton X-100 (T8200, Solarbio) at room temperature for 2 h. Incubated with iNOS Antibody (C-11) (sc-7271, SANTA CRUZ ANIMAL HEALTH, 1: 200), Anti-ki67 (ab16667, Abcam, 1:2000), Tenascin-C Monoclonal antibody (1F7G8, proteintech, 1:200), Anti-Collagen I antibody (ab270993, abcam, 1:2000) overnight at 4 °C. Subsequently, they were incubated with fluorescent secondary antibodies for 1 h. Finally, the cells were incubated with DAPI (1:200, c0060, Solarbio) for 10 min. The cells were photographed using a confocal fluorescence microscope (Leica SP8). Image J was used to analyze the positive expression.

Animal Culture: The experimental subjects were 63 SD rats (male, 8 weeks old, ≈250 g) without any disease. The rats were kept in the animal center of Beijing Institute of Nanoenergy and Nanosystems in a pathogen-free environment at 25 °C. General anesthesia and analgesia procedures were administered according to the Experimental Animal Guide provided by the Animal Resources Committee. All experimental procedures were reviewed and approved by the University Animal Resources Committee (2023031LZ), and followed the ARRIVE guidelines.

Biocompatibility in Vivo: 9 SD rats were randomly divided into three groups and injected with 200 µL IAH, PLLA (5 mg mL^{-1} in 1×PBS), and PE-IAH into the Achilles tendon by 1 mL syringe, respectively. Heart, liver, spleen, lung, and kidney of the SD rats were obtained on the 28th day, and these tissues were stained with hematoxylin and eosin (H&E) to obtain the biocompatibility of IAH, PLLA, and PE-IAH in vivo.

Animal Experiments: Rats were anesthetized by gas anesthesia using 2% isoflurane. The hair of the rat Achilles tendon was removed with electric hair clippers and depilatory cream. The skin of the Achilles tendon was incised, and the Achilles tendon was separated by a glass dissecting tool. The Achilles tendon was cut at the center of the transition between the Achilles tendon and the bone and the transition between the Achilles tendon and the muscle (Figure S18, Supporting Information). The Achilles tendon was sutured using the modified Kessler suture, and then the skin was sutured.

The 54 SD rats were randomly divided into 6 groups: Blank group (suture only), IAH group (200 µL IAH), PLLA-IAH group (200 µL IAH containing PLLA short fibers), US-IAH group (200 µL IAH + 20 min day^{-1} US), PE group (200 µL 1×PBS solution containing 5 mg ml^{-1} annealed PLLA short fibers + 20 min day^{-1} US), and PE-IAH group (200 µL PE-IAH + 20 min day^{-1} US). The frequency of US was 1 MHz, the power was 0.5 W cm^{-2}, and the duty cycle was 50%. IAH, PLLA, and PE-IAH were injected via a 1 mL syringe. All materials were sterilized by pasteurization. IAH, PE-IAH and PLLA short fibers in 1×PBS were injected by 1 mL syringe (needle inner diameter 0.33 mm). The duration of US treatment was 2 weeks, with treatments in 2-days-US and 1-day-rest pattern, for a total of 10 days. The paw prints of the rats during exercise were collected on the 2nd, 8th, and 14th days.[35] The Achilles tendon morphology was observed and recorded with a digital camera on the 8th day. The tendon tissue was taken for pathological sections on the 3rd, 8th, 14th, and 28th days.

Histology: The obtained tissues were fixed with 4% paraformaldehyde, dehydrated with graded ethanol, embedded in paraffin, and sliced at a thickness of 4 µm. The slices were analyzed by H&E, Masson, immunohistochemistry, and immunofluorescence staining. After microscopic observation, they were analyzed by Image J.

Antibodies: CD206/Mannose receptor/MMR antibody (15-2) (sc-58986, SANTA CRUZ ANIMAL HEALTH, 1: 100), iNOS Antibody (C-11) (sc-7271, SANTA CRUZ ANIMAL HEALTH, 1: 100), Anti-ki67 (ab16667, Abcam, 1:200), Tenascin-C Monoclonal antibody (1F7G8, proteintech, 1: 400), Anti-Collagen I antibody (ab270993, abcam, 1: 200)

Statistical Analysis: The statistical significance of the differences was determined by one-way ANOVA. All cell experiments were repeated three times. The statistical data of H&E staining, Masson staining, immunofluorescence staining, and immunohistochemistry staining of Achilles tendon tissue were obtained from parallel experiments of 3 rats. The data were analyzed using the mean ± standard error of the mean (S.E.M.) in GraphPad Prism v.8. Data were rendered using Image J (Media Cybernetics, USA) and Origin (OriginPro 2018C, OriginLab Corporation, USA). * $p < 0.05$, ** $p < 0.01$, *** $p < 0.001$ were considered statistically significant.

Supporting Information

Supporting Information is available from the Wiley Online Library or from the author.

Acknowledgements

The authors were grateful to all the laboratory members for their cooperation in this study. The authors thanks for the support received from National Key R&D Program of China (2022YFB3804700), National Natural Science Foundation of China (No. 82322037, T2125003), Beijing Natural Science Foundation (L245015), and the Fundamental Research Funds for the Central Universities.

Conflict of Interest

The authors declare no conflict of interest.

Data Availbility Statement

The data that support the findings of this study are available from the corresponding author upon reasonable request.

Keywords

injectable anti-adhesive hydrogel, piezoelectric stimulation, tendon adhesion, tendon repair

Received: January 18, 2025
Revised: July 4, 2025
Published online:

[1] A. Cretnik, R. Kosir, *J. Int. Med. Res.* **2023**, *51*, 03000605231205179.
[2] Y. H. Yeo, S. Kyeong, M. H. Kim, S. J. Lee, S. Y. Han, M. H. Park, D. Y. Kim, D. Y. Kim, I. Ha Yoo, C. Kang, J. H. Song, W. H. Park, *Int. J. Biol. Macromol.* **2024**, *271*, 132564.
[3] B. Kheilnezhad, A. Hadjizadeh, *Biomater. Sci.* **2021**, *9*, 2850.
[4] Y. Li, C. Hu, B. Hu, J. Tian, G. Zhao, C. Cai, Y. Li, Z. Sun, S. Wang, S. Pang, R. Bao, Z. Tao, H. Chen, J. Wu, S. Liu, *Adv. Healthcare Mater.* **2023**, *12*, 2203078.
[5] R. Wu, S. Pang, W. Lv, J. Zou, Y. Li, Y. Li, J. He, H. Gu, Y. Wang, Y. Guan, X. Peng, Y. Wang, S. Liu, *Adv. Funct. Mater.* **2024**, *34*, 2314731.
[6] a) Y. Xiao, Z. Tao, Y. Ju, X. Huang, X. Zhang, X. Liu, P. A. Volotovski, C. Huang, H. Chen, Y. Zhang, S. Liu, *Nano-Micro Lett.* **2024**, *16*, 186; b) S.-H. Chen, C.-H. Chen, Y. T. Fong, J.-P. Chen, *Acta Biomater.* **2014**, *10*, 4971; c) J. N. Li, X. R. Feng, B. C. Liu, Y. J. Yu, L. M. Sun, T. J. Liu, Y. H. Wang, J. X. Ding, X. S. Chen, *Acta Biomater.* **2017**, *61*, 21; d) J. Liao, X. Li, Y. Fan, *Bioact. Mater.* **2023**, *26*, 387.
[7] C. H. Lee, F. Y. Lee, S. Tarafder, K. Kao, Y. Jun, G. Yang, J. J. Mao, *J. Clin. Invest.* **2015**, *125*, 2690.
[8] T. Harvey, S. Flamenco, C.-M. Fan, *Nat. Cell Biol.* **2019**, *21*, 1490.
[9] a) N. L. Leong, J. L. Kator, T. L. Clemens, A. James, M. Enamoto-Iwamoto, J. Jiang, *J. Orth. Res.* **2020**, *38*, 7; b) S. Ruiz-Alonso, M. Lafuente-Merchan, J. Ciriza, L. Saenz-del-Burgo, J. L. Pedraz, *J. Controlled Release* **2021**, *333*, 448; c) Y. J. No, M. Castilho, Y. Ramaswamy, H. Zreiqat, *Adv. Mater.* **2020**, *32*, 1904511; d) L.-J. Ning, Y.-J. Zhang, Y. Zhang, Q. Qing, Y.-L. Jiang, J.-L. Yang, J.-C. Luo, T.-W. Qin, *Biomaterials* **2015**, *52*, 539.
[10] a) M. A. Fernandez-Yague, A. Trotier, S. Demir, S. A. Abbah, A. Larranaga, A. Thirumaran, A. Stapleton, S. A. M. Tofail, M. Palma, M. Kilcoyne, A. Pandit, M. J. Biggs, *Adv. Mater.* **2021**, *33*, 2008788; b) N. Saveh-Shemshaki, M. A. Barajaa, T. Otsuka, E. S. Mirdamadi, L. S. Nair, C. T. Laurencin, *Regen. Biomater.* **2023**, *10*, rbad099.
[11] a) X. Cui, L. Xu, Y. Shan, J. Li, J. Ji, E. Wang, B. Zhang, X. Wen, Y. Bai, D. Luo, C. Chen, Z. Li, *Sci. Bull.* **2024**, *69*, 1895; b) Y. Liu, G. Dzidotor, T. T. Le, T. Vinikoor, K. Morgan, E. J. Curry, R. Das, A. McClinton, E. Eisenberg, L. N. Apuzzo, K. T. M. Tran, P. Prasad, T. J. Flanagan, S. W. Lee, H. M. Kan, M. T. Chorsi, K. W. H. Lo, C. T. Laurencin, T. D. Nguyen, *Sci. Transl. Med.* **2022**, *14*, abi7282; c) M. Mirghaffari, A. Mahmoodiyan, S. Mahboubizadeh, A. Shahbazi, Y. Soleimani, S. Mirghaffari, Z. Shahravi, *Regenerat. Therapy* **2025**, *28*, 591.
[12] a) E. Murray, D. Challoumas, A. Putti, N. Millar, *J. Hand Surg. Am* **2022**, *47*, 896e1; b) F. R. Costa, M. R. C. Marques, V. C. Costa, G. S. Santos, R. A. Martins, M. d. S. Santos, M. H. A. Santana, A. Nallakumarasamy, M. Jeyaraman, J. V. B. Lana, J. F. S. D. Lana, *Biomedicines* **2023**, *11*, 1061.
[13] Q. Chen, X. Shao, P. Ling, F. Liu, G. Han, F. Wang, *Eur. J. Med. Chem.* **2017**, *139*, 926.
[14] Y. Tan, F. Han, S. Ma, W. Yu, *Carbohydr. Polym.* **2011**, *84*, 1365.
[15] A. E. C. Nichols, K. T. Best, A. E. Loiselle, *Transl. Res.* **2019**, *209*, 156.
[16] S. Chen, A. Saeed, Q. Liu, Q. Jiang, H. Xu, G. G. Xiao, L. Rao, Y. Duo, *Signal Transduction Targeted Ther.* **2023**, *8*, 207.
[17] M. Orecchioni, Y. Ghosheh, A. B. Pramod, K. Ley, *Front. Immunol.* **2019**, *10*, 1084.
[18] J. M. R. de la Rosa, A. Tirella, A. Gennari, I. J. Stratford, N. Tirelli, *Adv. Healthcare Mater.* **2017**, *6*, 1601012.
[19] T. Vinikoor, G. K. Dzidotor, T. T. Le, Y. Liu, H.-M. Kan, S. Barui, M. T. Chorsi, E. J. Curry, E. Reinhardt, H. Wang, P. Singh, M. A. Merriman, E. D'Orio, J. Park, S. Xiao, J. H. Chapman, F. Lin, C.-S. Truong, S. Prasadh, L. Chuba, S. Killoh, S.-W. Lee, Q. Wu, R. M. Chidambaram, K. W. H. Lo, C. T. Laurencin, T. D. Nguyen, *Nat. Commun.* **2023**, *14*, 6257.
[20] Y. Niu, F. J. Stadler, J. Fang, M. Galluzzi, *Colloids Surf., B* **2021**, *206*, 111970.
[21] a) M. C. B. Piedade, M. S. Galhardo, C. N. Battlehner, M. A. Ferreira, E. G. Caldini, O. M. S. de Toledo, *Ultra* **2008**, *48*, 403; b) G. R. Ebenbichler, C. B. Erdogmus, K. L. Resch, M. A. Funovics, F. Kainberger, G. Barisani, M. Aringer, P. Nicolakis, G. F. Wiesinger, M. Baghestanian, E. Preisinger, V. Fialka-Moser, *N. Engl. J. Med.* **1999**, *340*, 1533.
[22] S. Hajjar, X. Zhou, *Trends Immunol.* **2023**, *44*, 807.
[23] Y. Wang, S. Jin, D. Luo, D. He, C. Shi, L. Zhu, B. Guan, Z. Li, T. Zhang, Y. Zhou, C.-Y. Wang, Y. Liu, *Nat. Commun.* **2021**, *12*, 1293.
[24] a) G. S. Kryger, A. K. S. Chong, M. Costa, H. Pham, S. J. Bates, J. Chang, *J. Hand Surg. Am.* **2007**, *32A*, 597; b) D. J. Leong, H. B. Sun, *Ann. N. Y. Acad. Sci.* **2016**, *1383*, 88.
[25] D. A. Kaji, A. M. Montero, R. Patel, A. H. Huang, *Nat. Commun.* **2021**, *12*, 4208.
[26] a) Q. Zhang, Y. Yang, D. Suo, S. Zhao, J. C.-W. Cheung, P. H.-M. Leung, X. Zhao, *ACS Nano* **2023**, *17*, 16798; b) Z. Yin, J. J. Hu, L. Yang, Z. F. Zheng, C. R. An, B. B. Wu, C. Zhang, W. L. Shen, H. H. Liu, J. L. Chen, B. C. Heng, G. J. Guo, X. Chen, H. W. Ouyang, *Sci. Adv.* **2016**, *2*, 1600874.
[27] C. J. Dy, A. Hernandez-Soria, Y. Ma, T. R. Roberts, A. Daluiski, *J. Hand Surg. Am* **2012**, *37A*, 543.
[28] a) Z. J. Li, Q. Q. Yang, Y. L. Zhou, *Stem Cells Int.* **2023**, *2023*, 4387630; b) F. Jiang, H. Zhao, P. Zhang, Y. Bi, H. Zhang, S. Sun, Y. Yao, X. Zhu, F. Yang, Y. Liu, S. Xu, T. Yu, X. Xiao, *Front. Endocrinol.* **2024**, *15*, 1485876.
[29] C. N. Serhan, J. Savill, *Nat. Immunol.* **2005**, *6*, 1191.
[30] K. Kapat, Q. T. H. Shubhra, M. Zhou, S. Leeuwenburgh, *Adv. Funct. Mater.* **2020**, *30*, 1909045.
[31] a) A. Sindrilaru, K. Scharffetter-Kochanek, *Adv. Wound Care* **2013**, *2*, 357; b) M. L. Novak, E. M. Weinheimer-Haus, T. J. Koh, *J. Pathol.* **2014**, *232*, 344.
[32] C. Mondadori, A. Chandrakar, S. Lopa, P. Wieringa, G. Talo, S. Perego, G. Lombardi, A. Colombini, M. Moretti, L. Moroni, *Bioact. Mater.* **2023**, *21*, 209.
[33] a) R. N. Kent Iii, A. H. Huang, B. M. Baker, *Adv. Healthcare Mater.* **2024**, *13*, 2400668; b) C.-F. Liu, L. Aschbacher-Smith, N. J. Barthelery, N. Dyment, D. Butler, C. Wylie, *Tissue Eng. Part B Rev.* **2011**, *17*, 165.
[34] L. P. Malone, S. M. Best, R. E. Cameron, *Front. Bioeng. Biotechnol.* **2024**, *12*, 1419654.
[35] G. A. C. Murrell, E. G. Lilly, H. Davies, T. M. Best, R. D. Goldner, A. V. Seaber, *J. Orth. Res.* **1992**, *10*, 398.
[36] Y. Bi, D. Ehirchiou, T. M. Kilts, C. A. Inkson, M. C. Embree, W. Sonoyama, L. Li, A. I. Leet, B. M. Seo, L. Zhang, S. Shi, M. F. Young, *Nat. Med.* **2007**, *13*, 1219.